Plasma characteristics and quantitative analysis of Pb and Ni in soil based on LIBS technology*

LI Hong-lian (李红莲)[1,2]**, **WANG Hong-bao** (王红宝)[1,2], **HUANG Yi-chen** (黄一宸)[3], **KANG Sha-sha** (康沙沙)[1,2], **FU Shi-jie** (付士杰)[4], **LI Hao-ran** (李浩然)[1], **FANG Li-de** (方立德)[1,2], **and LI Xiao-ting** (李小亭)[1,2]

1. College of Quality and Technology Supervising, Hebei University, Baoding 071000, China

2. National and Local Joint Engineering Center of Measuring Instruments and Metrology Systems, Baoding 071000, China

3. College of Chemistry and Environmental Science, Hebei University, Baoding 071000, China

4. College of Optical Sciences, University of Arizona, Tucson 85721, America

(Received 8 November 2019; Revised 27 December 2019)

When measured by laser induced breakdown spectroscopy, the characteristic parameters of the plasma fluctuate significantly with the experimental parameters, which would have a greater impact on the quantitative measurement. The effects of two experimental parameters, lens to sample distance (*LTSD*) and delay time, on plasma temperature and electron density were analyzed. Thereafter the optimal *LTSD* and delay time for quantitative analysis of Pb and Ni in soil were identified. Two element calibration curves were calculated by the internal standard method under the optimal *LTSD* and delay time. About the two elements, correlation coefficient of the calibration curves is above 0.993. The maximum relative standard deviation (*RSD*) were 4.47% and 4.76%, respectively, and the maximum relative errors were 12% and 4.8%, respectively. The experimental results showed that laser induced breakdown spectroscopy method in combination with plasma characteristic parameter analysis shows the advantage on quantitative analysis of heavy metals in soil.

Document code: A **Article ID:** 1673-1905(2020)02-0143-6

DOI https://doi.org/10.1007/s11801-020-9189-8

Soil is an important aspect of the biosphere and the material basis and natural resources for human survival. Efficient, accurate and real-time detection of heavy metals in the soil is a basic requirement for modern precision detection technology. In some areas, both lead (Pb) and nickel (Ni) levels exceed the first level standard of national soil quality[1]. Pb and Ni in the soil can be gradually absorbed by plants, thus accumulated in the human body through food like vegetables and fruit, which threaten human health[2]. After decades of development, Laser induced breakdown spectroscopy (LIBS) technology has been widely used in the area of environmental monitoring, such as water pollution and soil pollution detection, as well as plant sample detection[3]. Compared with the common heavy metal detection methods (such as Inductively coupled plasma-atomic emission spectroscopy (ICP-AES), inductively coupled plasma mass spectrometry (ICP-MS), flame atomic absorption spectrometry (FLAA), etc.), the outstanding advantages of LIBS technology is simple, fast , sensitive and multiple elements can be analyzed online at the same time and multiple elements can be analyzed online at the same time[4]. In order to improve the detection accuracy of LIBS technology on heavy metal elements in soil, N. Ahmed et al[5] laser induced plasma spectroscopy (LIPS) with external magnetic field. To reduce the influence of matrix effect and improve measurement accuracy, Donaldson et al[6] simulated the process of LIBS technology to quantitatively analyze heavy metal elements in soil. Yin et al[7] uses a simplified standard addition method to improve the accuracy of LIBS technology for the detection of heavy metals in soil. J. Yongcheng et al[8] used LIBS technology and nonlinear multiple regression method to analyze the content of magnesium (Mg) in soil, where the ternary nonlinear regression is found to be the most suitable in the research model. It can effectively reduce the root mean square error and the relative error of the verification experiment.

When the plasma in the condition of local thermodynamic equilibrium, the wavelength and relative intensity of the plasma emission line mainly depend on the type, concentration, and plasma temperature of the element,

* This work has been supported by the Key Projects of Natural Science Foundation of Hebei Province (No.E2017201142), the 2018 Ministry of Education "Chunhui Program" Cooperative Scientific Research Projects, the Postdoctoral Research Projects in Hebei Province (No.B2016003008), and the Hebei Provincial Natural Science Youth Fund (No.D2012201115).

** E-mail: lihonglian@hbu.edu.cn

while the self-absorption and overlapping of the spectral lines affect the intensity distribution of the line. Therefore, when using LIBS technology for quantitative analysis, appropriate spectral lines should be selected to reduce the influence of self-absorption and spectral line overlap on the measurement results. In addition, the characteristic parameters of the plasma are accompanied by the plasma, which is very sensitive to the experimental conditions. The change of the measurement process affects significantly the quantitative measurement. Therefore, it is necessary to measure and analyze the spatiotemporal evolution characteristics of the plasma parameters[9]. Shaikh N M et al[10] studied the plasma characteristics of brass with the laser generated by the fundamental wave and the second and third harmonics of the yttrium aluminum garnet laser. Camacho et al[11] studied the plasma characteristic parameters of Ag atoms and Ag ions and found that continuous spectra and Ag ions decay faster than neutral Ag atoms. Yao et al[12] studied the spatial and temporal resolution evolution of pulse energy to femtosecond filament-assisted induction of heavy metal element plasma parameters in soil. It was found that with a gradual increase of delay time within 400 ns, the plasma temperature and electron density decreased rapidly. When increasing the distance away from the soil surface, soil plasma parameters increase first and then decrease. The above researchers have carried out research on the plasma characteristics of certain elements, but although the plasma characteristics of certain elements have been investigated in the above demonstrations, there are few reports on the application of plasma characteristics of research in quantitative analysis.

This paper analyzes the effects of delay time and lens to sample distance (*LTSD*) parameters on spectral signal strength and signal-to-noise ratio (*SNR*). The effects of these two experimental parameters on plasma temperature and electron density were also analyzed. The optimal *LTSD* and delay time for quantitative analysis of Pb and Ni in soil thus determined. Two element calibration curves were calculated by the internal standard method under the optimal *LTSD* and delay time.

The experiment was carried out with an Nd: YAG (type) pulsed laser at 532 nm as the excitation source. The maximum single pulse energy of the laser was 36 mJ, the pulse width was 8 ns, and the pulse repetition frequency was 6 Hz. The laser beam was focused by a lens with a focal length of 100 mm and function on the surface of the sample to generate a plasma signal. The signal was directly collected with the optical fiber and measured with a spectrometer (MX2500, Ocean Optics). The spectrometer obtains a wavelength measurement range of 200 nm to 960 nm and its highest resolution is 0.1 nm. The sample was placed on a rotating work platform. The schematic diagram of the experimental system is shown in Fig.1. The soil used in the experiment was standard soil (GBW07427), and the contents of Pb and Ni were 21.6 μg/g and 28.5 μg/g, respectively. The spectrally pure reagents PbO and Ni were then added to the standard soil to work as a standard sample of Ni and Pb. The contents of Ni in the standard soil samples were 0.07%, 0.1%, 0.25%, 0.4%, 0.7%, 0.9%, and 1.2%, respectively, and the Pb contents were 0.07%, 0.1%, 0.25%, 0.45%, 0.7%, 0.9% and 1.2%, respectively. Then a certain amount of saturated sucrose solution was added as a binder. After mixing from the fractions, the sample was processed with a 769YP-15A type powder tableting machine to achieve a raw sheet-like sample with a diameter of 15 mm and a thickness of 5 mm. The prepared soil samples were placed in a GZX-9070MBW digital blast drying oven at 80 °C for drying.

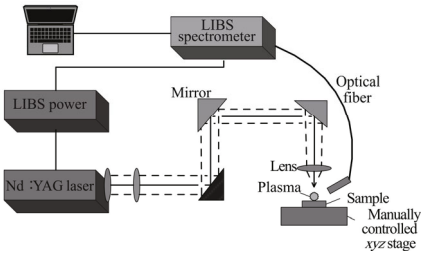

Fig.1 Schematic diagram of the experimental system

The intensity of the LIBS spectral signal is affected by the laser ablation area. The larger the ablation area, the more atoms that the sample is stripped and excited, and correspondingly, the greater signal can be achieved. However, when the laser energy is fix at a certain value, lower energy density induced by increased laser spot may compromise the breakdown capability. Therefore the experiment needs to optimize the parameter on *LTSD*[13,14]. The focal length of the lens used in this experiment is 100 mm, and the lens moves between focal plane positions of −8 mm to 0 mm. The distance from the lens to the sample is 92 mm-100mm. Fig.2 is a partial enlarged view of the spectrum in a wavelength range of 270 nm to 310 nm. As shown in Fig.2, as the distance of the lens to the focal plane changes, the spectral intensity increases at first and then decreases gradually. The *SNR* and *LTSD* curves of three elements Pb I 280.19 nm, Fe I 309.27 nm and Ni I 373.68 nm in soil are shown in Fig.3. The maximum *SNR* of Pb and Ni was achieved at a distance of 4 mm above the focal plane, the *LTSD* was 96 mm. and the distance to achieve maximum *SNR* of Fe should be tuned to 5 mm above the focal plane, the *LTSD* was 95 mm. Therefore, for comprehensive analysis, the distance from the lens to the surface of the sample is preferably 96 mm in this experiment.

The *SNR* calculation formula is expressed as

$$SNR = \frac{I - I_{\mathrm{B}}}{I_{\mathrm{B}}}, \tag{1}$$

where I is the line intensity, and I_{B} is the background signal strength of the spectrum. The background signal selects the average value of the background signals in the range of 1 nm from the left and right of the characteristic

spectrum.

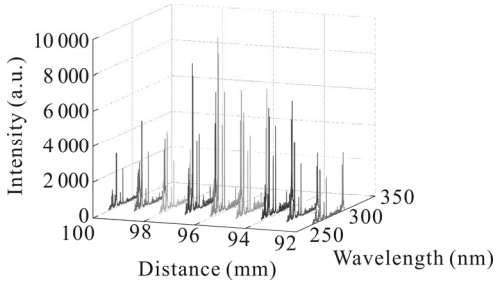

Fig.2 Effect of *LTSD* on spectral signal strength

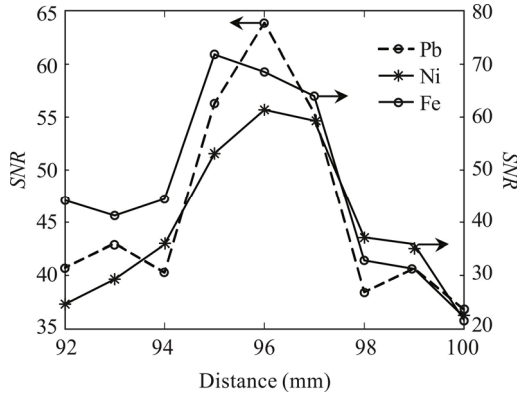

Fig.3 Spectral signal *SNR* change with *LTSD*

Plasma temperature and electron density are two important parameters to understand the plasma process. So the evolution of plasma temperature and electron density in function of the distance from the focus lens to the sample surface was calculated. In the condition of local thermodynamic equilibrium, five Fe atom spectral lines of Fe I 432.576 nm, Fe I 404.58 nm, Fe I 406.35 nm, Fe I 430.79 nm, Fe I 438.35 nm are selected and their peak emission intensities of the lines were used to calculate the electron temperature. The Boltzmann plot for calculation the electron temperature is shown in Fig.4. The related parameters of the five spectral lines are shown in Tab.1. where λ, E_k, A, g and I are the line wavelength, upper level energy, transition probability, statistical weight of the upper level, and line intensity, respectively.

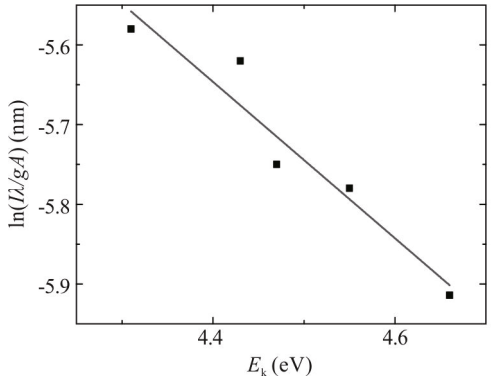

Fig.4 Boltzmann slash corresponding to the Fe line

Tab.1 Spectral parameters of three lines of Fe I atoms

λ (nm)	E_k (eV)	$A \cdot g$ ($\times 10^8$ s^{-1})
404.581	4.55	7.76
406.359	4.61	4.66
430.790	4.43	3.04
432.576	4.47	3.61
438.354	4.31	5.50

Fig.5 shows that the plasma temperature and electron density change with the distance of the focus lens to the sample surface, and the overall appearance shows a tendency to increase first and then decrease. And it has a maximum value of the plasma temperature and electron density at the distance of 4 mm above the focal plane, the *LTSD* was 96 mm.

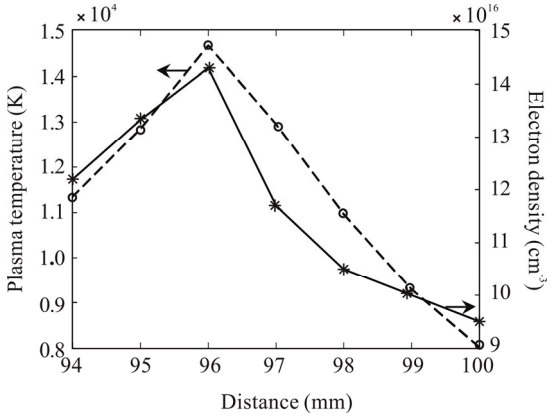

Fig.5 Plasma temperature and electron density changing with *LTSD*

When the distance of the lens-to-sample surface was reduced from 100 mm to 96 mm, the plasma temperature rose from 4 737 K to 4 757 K. The electron density increased from 9.5×10^{15} cm^{-3}to 14.3×10^{15} cm^{-3}. The minimum spot area is achieved when the distance from the lens to the sample is equal to the focal length, where the laser energy density is the largest. As the distance from the lens to the sample decreases, the spot area increases gradually. The number of atoms that are stripped and excited in the sample increases correspondingly, and the electron density grows up. The plasma temperature also gradually increases. As the spot area increases, the energy density gradually decreases. When the spot area increases to a certain value, the energy density ablation ability gradually decreases. The excited plasma in the sample is gradually reduced. Plasma temperature and electron density also decrease[4]. Therefore, when the distance from the lens to the sample is decreased from 96 mm to 94 mm, the plasma temperature is also reduced from 4 757 K to 4 666 K. The electron density was reduced from 14.3×10^{15} cm^{-3} to 12.2×10^{15} cm^{-3}. The electron density of the plasma is calculated by the full width

at half maximum $\Delta\lambda_{1/2}$ of the line, with a formula shown below[15]:

$$\Delta\lambda_{1/2}=2\omega\frac{N_e}{10^{16}}, \quad (2)$$

where ω is an electron collision parameter, ω is 0.176 at electron temperature of 10^4 K[16], and N_e is an electron density.

Eq.(3) is a condition for satisfying the local thermodynamic equilibrium, which requires that the plasma electron density N_e satisfies McWhirter standard.

$$N_e \geq 1.6\times10^{12}\Delta E^3 T_e^{1/2} \quad , \quad (3)$$

where N_e is electron density in cm^{-3} unit, T_e is plasma temperature in K unit, and ΔE in eV unit is the difference of upper and lower energy levels. In calculating the electron temperature, the maximum ΔE =3.1 eV. As shown in Fig.5, in the experiment, the highest electron temperature T_e=1.46×10^4 K. The calculated electron density N_e is 5.7×10^{15} cm^{-3} which is lower than the electron density 9.5×10^{15} cm^{-3} calculated by stark broadening of spectral line. Therefore, the local thermodynamic equilibrium assumption is effective.

In summary, the optimal *LTSD* is 96 mm. The plasma temperature, electron density, and *SNR* reached a maximum at an *LTSD* of 96 mm. Meanwhile, to achieve the plasma in local thermodynamic equilibrium, the optimal *LTSD* should be 96 mm.

The Pb I 280.19 nm, Fe I 309.27 nm, and Ni I 373.68 nm spectra were measured for different delay times. Fig.6 shows the relationship between the line intensity of the measured samples and delay time. As shown in Fig.6, during 0—3 μs delay time, the spectral intensity gradually decreases with increase of delay time. Fig.7 shows the trend in *SNR* of three elements with delay time. The intensity of the continuous background spectrum would gradually decrease with the increase of delay time. The effect of the continuous background spectrum on the atomic emission spectrum can be reduced by a time-resolved method. The optimum delay time is obtained at the maximum *SNR* of the atom-specific line. As shown in Fig.7, the spectral *SNR* of Pb I 280.19 nm and Ni I 373.68 nm exhibits a trend of increasing first and then decreasing at a delay time of 0—3.0 μs. When the delay time t_d=1.2 μs, the spectral *SNR* of the two elements reaches maximum. The Fe I 309.27 nm *SNR* gradually increased from 0 to 3.0μs and reached a maximum at 3.0 μs. The Pb and Ni elements have the largest spectral *SNR* at 1.2 μs, so the delay time is set to 1.2 μs.

The plasma generation process is mainly divided into three stages: a breakdown stage, an expansion stage, and a local stage. When the entire plasma in the condition of local thermodynamic equilibrium, the atoms or ions in the plasma at this time satisfy the Boltzmann distribution. The content of all atoms or ions in the plasma can be inferred according to the excitation number density of atomic or ion. The excitation number density of atoms or ions during the detection process can be obtained by detecting the spectral information of the plasma. Therefore, the specific information on the content of elements contained in the plasma body can be found from the plasma spectrum only when the plasma in the condition of local thermodynamic equilibrium.

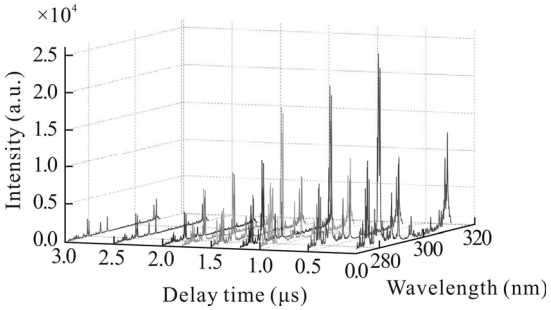

Fig.6 Effect of delay time on spectral signal strength

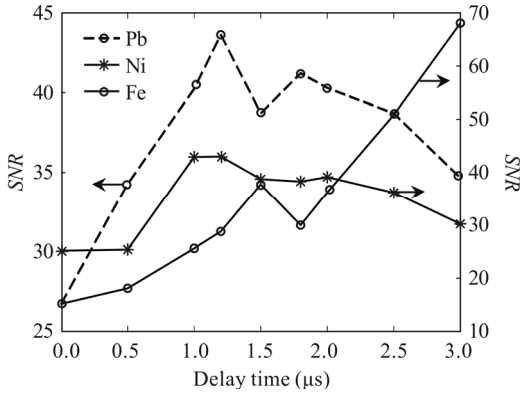

Fig.7 Spectrum signal *SNR* change with delay time

When the optimum delay time is determined by the spectral *SNR*, the *SNR* is maximized at a delay time of 1.2 μs. At this time, the continuous background light is the smallest, the characteristic line intensity is the largest, and a large amount of characteristic spectrum information is included. the relationship between delay time to plasma temperature and electronic density were analyzed. As shown in Fig.8, the plasma temperature and the electron density was gradually decreases as the delay time increases in the range of 1.2—3.0 μs.

As shown in Fig.8, the highest electron temperature was calculated in the experiment T_e=1.89×10^4 K. The electron density calculated by Eq.(2) was 6.56×10^{15} cm^{-3}, which was lower than the minimum electron density calculated by the Stark broadening method of 10×10^{15} cm^{-3}. Therefore, the local thermodynamic equilibrium assumption is effective. And plasma in the condition of local thermodynamic equilibrium at 1.2 μs, so the optimum delay time can be determined to be 1.2 μs.

After the above basic experimental research, the

optimized experimental conditions were: laser pulse energy of 36 mJ, delay time of 1.2 μs, and *LTSD* of 96 mm. Each sample took 5 different positions, and each spectrum is the average of 10 excitation signals, each point collection of 10 sets of spectral signals. To collected characteristic lines from soil standard samples containing Pb and Ni concentrations of 0.07%, 0.1%, 0.4%, 0.7%, and 0.9%. the calibration curves of Pb I 280.19 nm and Ni I 373.68 nm were established by the line intensity ratio. Fe I 309.27nm was used as the internal standard line. Fe I 309.27 nm was not the resonance line, which avoided the influence of self-absorption and ensure the stability of the spectral signal strength; At the same time, the upper and lower energy levels of the line are close to the upper and lower energy levels of Pb I 280.19 nm and Ni I 373.68 nm, so as to ensure that they have similar excitation states. Fig.9 shows the calibration curve established by the internal standard method of Pb and Ni in soil. The correlation coefficient R^2 of the calibration curve of Pb is 0.993, and the correlation coefficient R^2 of the calibration curve of Ni is 0.998. By calculating the maximum relative standard deviation (*RSD*) of Pb and Ni, which are 4.47% and 4.76%, respectively, it can be seen that the correlation coefficient of the two element calibration curves is relatively high and has certain utilization value.

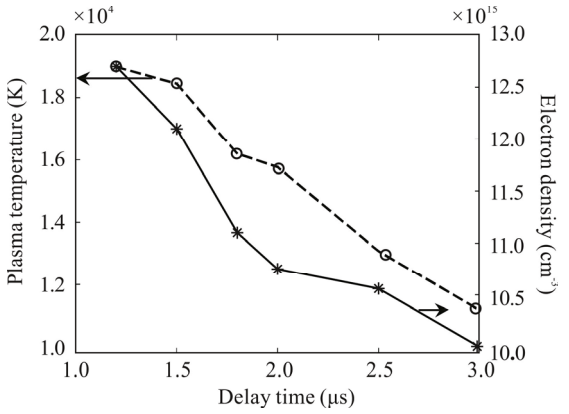

Fig.8 Plasma temperature and electron density change with delay time

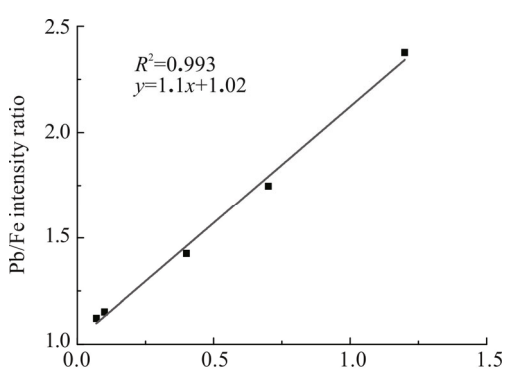

(a) Pb element

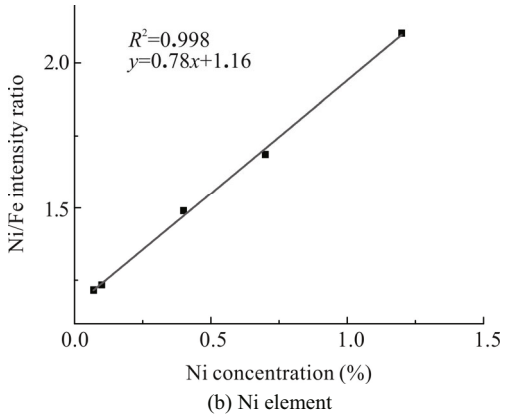

(b) Ni element

Fig.9 Calibration curves of Pb and Ni elements in soil

Quantitative analysis of soil samples (0.25%, 0.9%) was performed under optimized experimental conditions, and 50 spectra were also collected for each sample. Pb I 280.19 nm and Ni I 373.68 nm were selected as analytical lines. The results show in Tab.2 that the relative error of Pb content in internal standard method is 12% and 5.5%, and the relative error of Ni content is 4.8% and 1.1%.

Tab.2 Results of quantitative analysis of Pb and Ni

	Standard concentration	Fitting inversion concentration	Relative error
Pb	0.25%	0.28%	12%
	0.9%	0.85%	5.5%
Ni	0.25%	0.238%	4.8%
	0.9%	0.89%	1.1%

In this experiment, a method of optimizing the experimental conditions by combining the *SNR* of the spectral signal with the characteristic parameters of the plasma is used. Compared with some methods in recent reports, the relative error is reduced. Wu[7] used the standard addition method to quantitatively analyze the Pb in the soil using LIBS, with a maximum relative error of 29%. Fang[17] used the standard addition method to quantitatively analyze the Pb in the soil, and the maximum relative error was 38.3%. Zheng[18] used the heating double pulse method to quantitatively analyze Pb in Coptis chinensis with a maximum relative error of 13.2%. In recent reports, the maximum relative error range is between 13.2% and 38.3%. This experiment reduces the maximum relative error to 12% and improves the detection accuracy.

Quantitative analysis of two elemental components of Pb and Ni in soil was achieved based on laser induced breakdown spectroscopy. The relationship between *LTSD*, delay time and plasma characteristic parameters was analyzed. The optimum *LTSD* was determined to be 96mm and the optimum delay time was 1.2 μs. The

internal standard method was used to quantitatively analyze lead and nickel in soil samples. The experimental results show that the linear correlation coefficient R^2 of the Pb calibration curve was 0.993 and the linear correlation coefficient R^2 of the Ni calibration curve was 0.998. the maximum *RSD* of the two elements was 4.47% and 4.76%, respectively. It is proved that the line intensity has a good linear relationship with the element concentration. The maximum relative error of Pb content was less than 12%, and the maximum relative error of Ni content was less than 4.8%. In the quantitative analysis of soil samples, it is important to select the appropriate experimental parameters. Consideration should be given to the variation of the plasma characteristic parameters with experimental parameters. Thereby determining the optimal experimental conditions.

References

[1] Bai Jun-hong, Zhao Qing-qing, Lu Qiong-qiong, Wang Jun-jing and Ye Xiao-fei, Journal of Wetland Science **11**, 271 (2013). (in Chinese)

[2] Akhtar M., Jabbar A., Mahmood S., Umar Z. A. and Baig M. A., Analytical Letters **52**, 1 (2019).

[3] Peter D. I., Jamie R. N., Elizabeth H. D., Joshua J. R., Eirik J. K., Ryan S. R. and James J. M., Soil Biology and Biochemistry **131**,119 (2019).

[4] Chatterjee S., Singh M., Biswal B. P., Sinha U. K., Patbhaje S. and Sarkar A, Analytical and Bioanalytical Chemistry **411**, 2855 (2019).

[5] Akhtar M., Jabbar A., Ahmed N., Mahmood S., Umar Z. A., Ahmed R. and Baig M. A., Applied Physics B **125**, 110 (2019).

[6] Donaldson K M and Yan X T., Geoderma **337**, 701 (2019).

[7] C. Wu and D. X. Sun, Royal Society of Chemistry **34**, 1478 (2019).

[8] Yongcheng J., Wen S., Baohua Z. and Dong L., Journal of Applied Spectroscopy **84**, 731 (2017).

[9] Singh K. S and Sharma A. K., Physics of Plasmas **23**, 123514 (2016).

[10] Shaikh N. M., Hafeez S., Kalyar M. A., Ali R. and Baig M. A, Journal of Applied Physics **104**, 103108 (2008).

[11] Camacho J. J., Oujja M., Sanz M., Martínez-Hernández A., Lopez-Quintas I. and De Nalda, R, Imaging Spectroscopy of Ag Plasmas Produced by Infrared Nanosecond Laser Ablation, Journal of Analytical Atomic Spectrometry **34**, 2019.

[12] Yao Shuang, Zhang Jing, Gao Xun, Zhao Shang-yong and Lin Jing-quan, Optics Communications **425**, 152 (2018).

[13] Wang Tao, He Ming-jiang, Shen Ting-ting, Liu Fei, He Yong, Liu Xing-mei and Qiu Zheng-jun, Spectrochimica Acta Part B: Atomic Spectroscopy **149**, 300 (2018).

[14] Zhang Dan, Chen An-ming, Wang Qiu-yun, Li Su-yu, Jiang Yuan-fei and Jin Ming-xing, Plasma Science and Technology **21**, 73 (2019).

[15] Meng De-shuo, Zhao Nan-jing, Ma Ming-jun, Fang li, Gu Yan-hong, Jia Yao, Liu Jian-guo and Liu Wen-qing, Applied Optics **56**, 5204 (2017).

[16] N. Konjevic, A. Lesage, J.R. Fuhrand and W. L. Wiese, J. Phys. Chem. Ref. Data **31**, 819 (2002).

[17] Fang Li, Zhao Nan-jing, Ma Ming-jun, Meng De-shuo, Gu Yan-hong, Jia Yao, Liu Wen-qing and Liu Jian-guo, Spectroscopy and Spectral Analysis **37**, 3274 (2017).

[18] Zheng Pei-chao, Li Xiao-juan, Wang Jin-mei, Zhen Shuang and Zhao Huan-dong, Acta Phys. Sin. **68**, 125202-1(2019). (in Chinese)